

# Nature and Source of Organic Matter in the Shoemaker–Levy 9 Jovian Impact Blemishes

Peter D. Wilson and Carl Sagan†

*Laboratory for Planetary Studies, Cornell University, Ithaca, New York 14853-6801*

E-mail: wilson@astrosun.tn.cornell.edu

Received June 14, 1996; revised May 22, 1997

The 0.3–1.0  $\mu\text{m}$  optical constants of the aerosols in the dark SL-9 Jupiter impact blemishes are nearly identical to those of the organic residue in the Murchison carbonaceous chondrite. Porous poly-HCN is also a reasonable match. The mass of organics needed to produce a typical blemish is  $0.8\text{--}8 \times 10^{13}$  g, depending on the aerosol porosity. The 10  $\mu\text{m}$  emission feature seen during the splash-back phase for the impact of fragment R, however, requires  $\sim 1\text{--}5 \times 10^{12}$  g of astronomical silicate. The organics from the blemishes cannot be present at this point, or else its greater abundance would dominate the thermal flux, hiding or greatly modifying the 10  $\mu\text{m}$  silicate feature. Furthermore, this mass of silicates, but not the mass of organics in the blemishes, is consistent with the HST reflectances of the impact plumes if the aerosols have radii  $\sim 0.1 \mu\text{m}$ .

In addition to the blemishes, a large expanding ring was observed for the G and K impacts between 3 and 4  $\mu\text{m}$  but was not detected outside that range. Titan tholin has a strong absorption edge near 3  $\mu\text{m}$  which decays by a factor of 8 by 4  $\mu\text{m}$ . Poly-HCN and Murchison organic residue have similar but less extreme behavior. If the radiation from the ring is thermal emission instead of reflected sunlight, this feature is best explained by a very thin cloud of hot Titan tholin-like aerosols at the few microbar level. The rings require  $\sim 10^{10}$  g of material.

The mass of organics required to produce the blemishes is comparable to the organic abundance expected in the  $\sim 10^{14}$ -g fragments, assuming cometary composition. However, the high temperature of the fireball would likely destroy most, if not all, of the organic matter contained within the fragments. Because of the low abundance of HCN seen at the impact sites, shock synthesis of organics from the jovian atmosphere is an improbable production mechanism. Quench synthesis of organics from cometary dissociation products, though, may satisfy the large mass requirements. The expanding ring requires a low enough mass of tholin that the latter is reasonably the result of shock synthesis, possibly during the splash-back phase. © 1997 Academic Press

## INTRODUCTION

The whole world watched as  $\sim 20$  separate fragments of Comet Shoemaker–Levy 9 crashed into Jupiter in the summer of 1994. Observations were made of every phase of the impacts, from entry to debris dispersal. Deciphering all the data and building a consistent picture of the many phenomena seen is a major undertaking likely to continue for many more years, if not decades. One small piece of the puzzle are the aerosols.

The impacts sent large volumes of hot gas and vapor thousands of kilometers above Jupiter's clouds. The Hubble Space Telescope was able to resolve these plumes and determine that they were weakly reflecting sunlight (Hammel *et al.* 1995). Solid material was clearly present. When the plume fell back into Jupiter's atmosphere, the plume material was again reheated, producing the strongest peak in the infrared lightcurves of the impacts. In the best-studied splash-back event, impact R, solid silicate emission was detected (Nicholson *et al.* 1995b).

When Jupiter had rotated enough to bring the impact sites into view, most of them were surrounded by blemishes which appeared dark in the visible and ultraviolet, but bright within methane absorption bands, indicating the presence of aerosols well above Jupiter's clouds. The general trend was for the brighter (and presumably larger) fragments to produce larger and more complex blemishes (Hammel *et al.* 1995). The smallest fragments produced no atmospheric features while the largest fragments made a complex pattern consisting of one or two expanding rings  $\sim 1500\text{--}4500$  km in radii, an interior triangular region extending from the center of the ring to its southeast edge, and an exterior  $180^\circ$  crescent extending  $\sim 6000\text{--}13,000$  km to the southeast of the ring center (Hammel *et al.* 1995).

Observations of the G and K impact sites in the infrared detected a bright ring expanding beyond the dark crescent (McGregor *et al.* 1996). The ring was seen at 3–4  $\mu\text{m}$  but not at shorter or longer wavelengths. The flux from the ring decreased with time until it faded into the background several hours after the impacts.

† Deceased December 20, 1996.

The composition, production mechanism, and evolution of the aerosols in each of the above stages are unsolved problems. The solutions may have implications for the composition of both Shoemaker–Levy 9 and the jovian atmosphere at the impact sites, as well as for the physics and chemistry of large airbursts. The primary possibilities suggested for composition are silicates, sulfur compounds, and organic matter (West *et al.* 1995). Nicholson *et al.* (1995b) successfully identified silicates in their observations of the splash-back phase, but West *et al.* (1995) found silicates incompatible with the observations of the blemishes. Indeed, none of the materials examined by West *et al.* appeared viable. Here we consider the ability of organic matter—either delivered by the cometary fragments (intact or reprocessed in the fireball) or synthesized in airburst shock waves—to explain the observations of each phase of the impact, trying to tie together our results into a consistent picture.

### BLEMISH AEROSOL COMPOSITION

Several groups have modeled the scattering properties of the Jupiter blemishes and estimated the imaginary part,  $k$ , of the complex refractive index,  $m$ , of the aerosols: West *et al.* (1995) derived  $k$  at 5 wavelengths in the range  $\lambda = 0.275\text{--}0.89\ \mu\text{m}$ ; Moreno *et al.* (1995) and Muñoz *et al.* (1996) independently confirmed the imaginary refractive index in the same wavelength range; Yelle and McGrath (1996) added a value for  $k$  at  $0.2\ \mu\text{m}$ ; Ortiz *et al.* (1995) added  $k$  at 1.7 and  $2.3\ \mu\text{m}$ ; and Rosenqvist *et al.* (1995) modeled their own and other's observations of the hazes to estimate  $k$  at 2.14, 3.9, and  $\sim 10\ \mu\text{m}$ . There appear to be problems with the Ortiz *et al.* and Rosenqvist *et al.* models, however. Ortiz *et al.* derived  $k$  from observations within deep methane absorption bands where scattered light is coming from the highest region of the haze which is extremely optically thin ( $\tau \leq 0.01$ ). Even for very absorbing particles, the methane will be absorbing 100 times as much radiation, so Ortiz *et al.* should not be able to place any constraints on  $k$  at these wavelengths. The  $2.14\ \mu\text{m}$  result of Rosenqvist *et al.* suffers the same problem and the  $3.9\ \mu\text{m}$  value comes from an uncalibrated observation. Given these problems and the fact that their  $10\ \mu\text{m}$  calculation of  $k$  cannot be confirmed because their reference is a 1995 DPS abstract which does not report the necessary observations, we have little trust in the  $10\ \mu\text{m}$  datum as well. We therefore reject the Rosenqvist *et al.*, as well as the Ortiz *et al.*, results entirely. For completeness, though, they are plotted with the other  $k$  values in Fig. 1.

Each group adopts or derives a particle radius  $\sim 0.15\text{--}0.3\ \mu\text{m}$  for the aerosols. Because the particles are comparable in size to the shorter wavelengths being modeled, their scattering and absorption behavior will be strongly dependent on particle size, shape, and structure. Modeling them

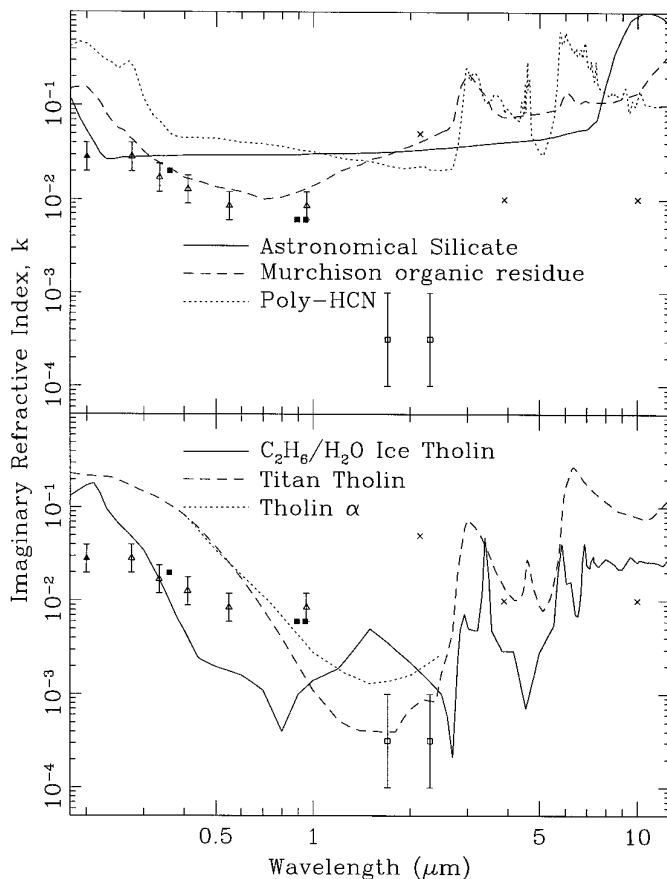


FIG. 1. The imaginary refractive indices of the blemishes compared to those of six materials from 0.2 to  $10\ \mu\text{m}$ . Blemish data longward of  $1\ \mu\text{m}$  are thought unreliable. Murchison residue provides the best fit to the visible data. In contrast, each tholin is too red; poly-HCN is too absorbing; and astronomical silicate is too neutral. [Solid triangle, Yelle and McGrath (1996); open triangles, West *et al.* (1995); solid squares, Moreno *et al.* (1995); open squares, Ortiz *et al.* (1995); crosses, Rosenqvist *et al.* (1995).]

with Mie scattering theory, which assumes homogeneous spheres, introduces systematic errors, so the uncertainties in  $k$  are likely larger than reported.

Comparison of the above models to several sulfur compounds and astronomical silicate and graphite reveals poor matches to  $k(\lambda)$  in both absolute value and wavelength dependence (West *et al.* 1995). Polymerized hydrogen cyanide (henceforth poly-HCN) crudely follows the visible wavelength-dependence but is too absorbing by a factor of  $\sim 3$  (West *et al.* 1995).

In Fig. 1, we compare the imaginary refractive indices of the aerosols to those of six astronomically interesting materials, including two atmospheric organic tholins, meteoritic organics, and astronomical silicate. Due to the difficulty of working in the laboratory with true jovian-like conditions, the production procedures for the organic sol-

ids do not accurately recreate the conditions expected during or after the SL-9 impacts. Our selection of materials is driven mostly by what is available, not by relevance of the production mechanisms.

Tholin  $\alpha$  is a dark organic solid produced by charged-particle irradiation of a gas of composition 3% CH<sub>4</sub>, 25% He, and 72% H<sub>2</sub> (Khare *et al.* 1987) and may resemble shock-synthesized organics produced in the jovian atmosphere. Its optical constants have been measured only over a narrow wavelength range (0.4–2.5  $\mu\text{m}$ ), so we include Titan tholin to represent all atmospheric tholins. Titan tholin is an organic solid made by plasma discharge through a 9:1 N<sub>2</sub>:CH<sub>4</sub> atmosphere, simulating the observed atmosphere of Titan. Titan tholin's optical constants (Khare *et al.* 1984) match within the probable error the ultraviolet, visible, and near- and middle-infrared spectrophotometry of Titan (Sagan *et al.* 1992). Ice tholin is the organic residue produced by charged-particle irradiation of a 1:6 C<sub>2</sub>H<sub>6</sub>:H<sub>2</sub>O ice mixture (Khare *et al.* 1993). Because ice tholin should resemble the residue from irradiated CH<sub>4</sub>/H<sub>2</sub>O mixtures (Khare *et al.* 1993), ice tholin may be abundant in comets. Murchison organic residue is the water-insoluble organic residue from the Murchison Type-II carbonaceous chondrite (Khare *et al.* 1990, Khare, B. N., C. Sagan, W. R. Thompson, E. T. Arakawa, C. Meisse, I. Gilmour, and P. S. Tuminello, in preparation). Murchison organics may represent the primordial organic matter from some mix of circumstellar, interstellar, nebular, and meteorite parent body processes accreted by both asteroids and comets (Khare *et al.*, in preparation). Poly-HCN is an organic solid produced from HCN and has been suggested to be widely distributed through the outer Solar System (Matthews 1992, Wilson *et al.* 1994, Wilson and Sagan 1995), including explicitly the dark blemishes on Jupiter (Matthews 1994). Astronomical silicate is a model of interstellar silicate grains derived from emission and absorption profiles of grains in molecular clouds and circumstellar dust shells (Draine and Lee 1984, Draine 1985). Although more accurate and complete refractive index data are available for terrestrial silicates (cf. Roush *et al.* 1991), these materials have 10  $\mu\text{m}$  absorption bands that are much narrower than that of astronomical silicate.

Murchison residue is by far the best match to most of the data, but is a factor of a few too absorbing at 0.2  $\mu\text{m}$ . An even better fit can be obtained by assuming porous aerosols which will lead to lower "effective" refractive indices. A 50% porosity (*i.e.*, internal void space) would be ideal and easily obtained by the coagulation of small 0.1  $\mu\text{m}$  particles to form the observed 0.15–0.3  $\mu\text{m}$  aerosols. Porous poly-HCN aerosols would likewise counter poly-HCN's greater absorption, but the porosity would need to exceed 80% to do as well as Murchison residue. Porosity will also lower the real part,  $n$ , of the aerosols' refractive index which will alter their scattering properties. For the

desired porosities of Murchison and poly-HCN aerosols,  $n \approx 1.1$ –1.2. The aerosol models have all assumed  $n = 1.4$  or 1.7. It is unclear whether the significantly lower values of  $n$  would in turn significantly affect the modeled values of  $k$ .

None of the tholins come close to matching the data—they all have too steep a slope in the visible.

The volume of the aerosols has been calculated by West *et al.* (1995) and Banfield *et al.* (1996), but they obtained rather different values. Based on the optical depths of the haze measured in the visible, West *et al.* summed up all the aerosols from all the impacts, finding a total volume  $\sim 5.6 \times 10^{14} \text{ cm}^3$ . Banfield *et al.* did likewise for their observations in the near infrared, but in calculating the aerosol scattering efficiency, they mistakenly used the small- $n$  limit:  $(n - 1) \ll 1$ . Since they assumed aerosols with  $n = 1.4$  (from West *et al.*), they should have used the small-particle scattering equation for  $(n - 1) \approx 1$ . This results in a factor of 4 increase in their derived volume. Their total aerosol volume, when corrected, is  $\sim 4.4 \times 10^{15} \text{ cm}^3$ , nearly a factor of 10 greater than West *et al.*'s.

Light can be shed on this discrepancy, since Banfield *et al.* also reported the volumes of the aerosols in individual impact sites, so their values can be compared to the Moreno *et al.* (1995) model of the H impact site. Banfield *et al.* assumed 0.25  $\mu\text{m}$  aerosols with  $n = 1.4$ , whereas Moreno *et al.* assumed  $n = 1.7$  and derived an aerosol radius of 0.15  $\mu\text{m}$ . Using the Moreno *et al.* aerosol properties, Banfield *et al.*'s observations resulted in a mean particle density of  $2.4 \times 10^9 \text{ cm}^{-2}$  spread over an area of  $1.3 \times 10^{19} \text{ cm}^2$ , giving a total volume of  $4.4 \times 10^{14} \text{ cm}^3$ . Moreno *et al.* only looked at the core of the blemish, finding a particle density of  $8.2 \times 10^9 \text{ cm}^{-2}$ . Hammel *et al.* (1995) classified the H impact as medium-sized with a blemish extending out to 4000–8000 km. Given the arc's asymmetry and the absence of material between the core and arc, the blemish itself covers  $\leq 5 \times 10^{17} \text{ cm}^2$ . Although this is significantly smaller than the area measured by Banfield *et al.*, the latter observed several days later, by which time the blemish had spread due to winds. Applying Moreno *et al.*'s particle density from the core to the entire blemish, the maximum aerosol volume is  $\sim 6 \times 10^{13} \text{ cm}^3$ . This is much less than the Banfield *et al.* volume, but is consistent with the volume expected from West *et al.* for a medium-sized blemish. We thus reject Banfield *et al.*'s volume calculations.

Fifteen impactors produced observable blemishes (Hammel *et al.* 1995), so the average blemish contained  $\sim 4 \times 10^{13} \text{ cm}^3$  of aerosols. Organic solids have densities  $\sim 2 \text{ g cm}^{-3}$ . For porosities up to 90%, a typical blemish may contain  $\sim 0.8$ – $8 \times 10^{13} \text{ g}$  of material.

#### PLUME AEROSOL COMPOSITION

Nicholson *et al.* (1995a, 1995b) performed narrowband photometry at 3.2  $\mu\text{m}$ , broadband photometry at 3–5  $\mu\text{m}$ ,

and low-resolution spectroscopy at 8–13  $\mu\text{m}$  near the peak brightness of impact fragment R. Friedson *et al.* (1995) also obtained photometry of impact fragment R at 7.85, 10.3, and 12.2  $\mu\text{m}$ . Sprague *et al.* (1996) obtained additional spectra of the R-impact plume at 6–9  $\mu\text{m}$ . [These observations were obtained with the High Efficiency Faint Object Grating Spectrograph (HIFOGS) on the Kuiper Airborne Observatory (KAO). The spectra actually cover the region 4.8–9.5  $\mu\text{m}$ , but these data have not been published yet. The HIFOGS KAO observing team (Sprague *et al.* 1996) has supplied us with these additional data which we have included in sampled form in our modeling.] Graham *et al.* (1995), McGregor *et al.* (1996), and Meadows *et al.* (1995) also observed the R-impact plume at 2.3  $\mu\text{m}$ . Each of these sets of data is plotted in Fig. 2.

Several disagreements are present between different observation data sets. Graham *et al.* and Meadows *et al.* obtained peak brightnesses for 2.3  $\mu\text{m}$  that differ by a factor  $\sim 6$ . Graham *et al.* reported that their detector was being saturated during the  $\sim 5$  min surrounding peak brightness, but that they recovered photometry during this period by modeling the unsaturated pixels in the wings of the point-spread function. Although they are confident in their results, there is likely a sizable uncertainty in their reported peak brightness. McGregor *et al.* reported a flux in between those of Graham *et al.* and Meadows *et al.*, but, like Graham *et al.*, their detector was being saturated. McGregor *et al.* did not try to correct their measurements, however.

The spectra at peak brightness from Nicholson *et al.* (1995b) and Sprague *et al.* also differ by a factor  $\sim 3$  in the region of overlap: 8–9.5  $\mu\text{m}$ . Friedson *et al.*'s 7.85  $\mu\text{m}$  observation is  $\sim 40\%$  greater than Sprague *et al.*'s, and all their observations are 1.5–2 times lower than Nicholson *et al.*'s (1995b). The Nicholson *et al.* (1995b) spectrum was obtained at Palomar while Jupiter was near the horizon at an airmass  $\sim 3$ , whereas the Sprague *et al.* spectrum was taken on the KAO and the Friedson *et al.* observations were made at the IRTF in Hawaii. Due to an "ideally situated" standard star, Sprague *et al.* claimed an accuracy of a few percent in their absolute fluxes. Nicholson *et al.* (1995b) did not observe precisely at peak brightness, so they used the 3–5  $\mu\text{m}$  lightcurve from Nicholson *et al.* (1995a) to scale upward a spectrum taken 2 min before the peak. Sprague *et al.* compare their observations to the Nicholson *et al.* (1995a) 3–5  $\mu\text{m}$  lightcurve and find a slightly earlier time of peak brightness in their data, so the Nicholson *et al.* (1995b) correction may not have been necessary, or at least not correct. This correction, however, amounted to only  $\sim 65\%$ . Because the shapes of the spectra are more important than the absolute fluxes for modeling aerosol compositions, we rescale the Sprague *et al.* and Nicholson *et al.* (1995b) data to more or less coincide with the intermediate Friedson *et al.* data (see top of Fig. 2).

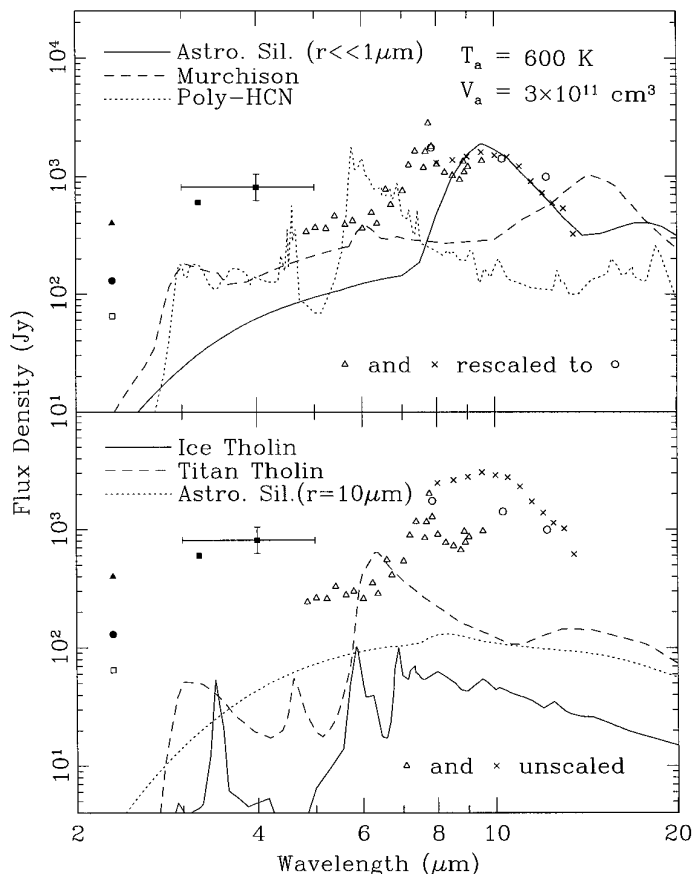


FIG. 2. Comparison of thermal emission from aerosols of five materials at 600 K and total volume  $3 \times 10^{11} \text{ cm}^3$  to peak flux observations of impact R. Emission from larger 10  $\mu\text{m}$  astronomical silicate particles is also plotted. Error bars are plotted only for the 4  $\mu\text{m}$  point to indicate that it is a broadband measurement and has a much larger calibration uncertainty than the other points. All the observations shortward of 5  $\mu\text{m}$  though are likely contaminated by methane gas emission. Only small astronomical silicate particles have a 10  $\mu\text{m}$  feature able to match the Nicholson *et al.* (1995b) data. None of the organic materials when added to the silicates improve the fit at other wavelengths. [Solid triangle, Meadows *et al.* (1995); solid circle, McGregor *et al.* (1996); open square, Graham *et al.* (1995); solid squares, Nicholson *et al.* (1995a); open triangles, Sprague *et al.* (1996) and A. Sprague (personal communication, 1997); open circles, Friedson *et al.* (1995); crosses, Nicholson *et al.* (1995b).]

This simply results in a factor  $\sim 2$  uncertainty in the aerosol volume present.

Using Hubble Space Telescope (HST), Hammel *et al.* (1995) observed the rise and collapse of the plumes for impacts A, E, G, and W. Assuming these were similar to the R-impact plume, the HST observations at the time of peak brightness in the infrared can provide an additional constraint on the thermal emission of the aerosols. Only the E-impact sequence used long enough filters ( $\lambda \approx 0.9 \mu\text{m}$ ) to be sensitive to the likely temperatures during the splash-back phase. The flux measured in one image was

$\sim 10^{-5}$  Jy and clearly due to reflected sunlight. A second image taken 3 min later was likely nearer the peak brightness, but the plume's brightness was not reported for this image. The second image is much brighter than the first, but part of this is because its exposure time was twice as long; a different filter was also used. Although uncertain, the plume's peak brightness at  $0.9 \mu\text{m}$  was probably not much greater than  $10^{-5}$  Jy. Thermal radiation from the aerosols needs to be less than this.

The observed radiation from the plume is not exclusively, nor possibly even primarily, due to solid particles. Hot gases in the plume will also radiate. Sprague *et al.* identify both  $\text{H}_2\text{O}$  ( $6.45$  and  $6.62 \mu\text{m}$ ) and  $\text{CH}_4$  ( $7.2$ – $8.2 \mu\text{m}$ ) line emission in their spectra. Methane will likewise be a strong emitter at  $2.3$  and  $3.3 \mu\text{m}$  which coincide with all the near-infrared observations listed above. These data, therefore, are poor constraints on possible aerosol properties. At best, assuming optically thin gas emission, which is suggested by the sharp peak of the  $7.7 \mu\text{m}$  methane band (i.e., the line is unsaturated), the observations below  $5 \mu\text{m}$  represent upper limits to aerosol emission. Further, because of the strength and width of the  $7.7 \mu\text{m}$  emission band and the additional presence of  $\text{H}_2\text{O}$  lines, most of the Sprague *et al.* spectrum may likewise be upper limits on continuum emission from the aerosols.

The thermal flux from an optically thin cloud of Rayleigh particles is given by  $F_\nu(\lambda, T_a) = \Omega \tau_g \varepsilon B_\nu(\lambda, T_a)$ , where  $\Omega$  is the solid angle of the emitting region,  $\tau_g$  is the mean geometric optical depth of the cloud, and  $\varepsilon$  is the emissivity which is equivalent to the Rayleigh absorption efficiency,  $Q_A$ . Because the emissivity depends (linearly) on particle size, we cannot solve for  $\tau_g$  independent of the particle radius,  $r$ . However, we can remove the particle size dependence in the flux calculation by relating  $\tau_g$  to the total aerosol volume:  $V_a = \frac{4}{3} r \tau_g \Omega \Delta^2$ , where  $\Delta = 8 \times 10^{13}$  cm is the Earth–Jupiter separation, giving

$$F_\nu(\lambda, T_a) = \frac{3V_a}{4\Delta^2} \frac{Q_A}{r} B_\nu(\lambda, T_a), \quad (1)$$

which, because  $Q_A \propto r$ , is independent of  $r$  for  $r \ll \lambda$ .

Nicholson *et al.* (1995b) have rather convincingly identified silicates in the plume. Because none of our organic materials have a  $10 \mu\text{m}$  emission feature, we treat silicate as a required material and fit it to the data first. At temperatures above  $600$  K, the flux from silicate grains will exceed the flux seen by HST at  $0.9 \mu\text{m}$ . Below  $\sim 350$  K, the fit to the  $10\text{-}\mu\text{m}$  feature becomes very poor. The aerosol volumes required at these two temperatures are  $3 \times 10^{11}$  and  $1.6 \times 10^{12}$   $\text{cm}^3$ , respectively. Figure 2 plots the thermal spectra of the materials from Fig. 1 (except for tholin  $\alpha$ ) at  $600$  K. For easy comparison the silicate volume is also used for the organic materials.

The aerosol volume and spectra are calculated assuming

Rayleigh particles. This may not be the case for the silicates. For a high enough silicate concentration, West *et al.* (1995) expect silicates to condense out of the cooling fireball and plume with particle sizes of  $10 \mu\text{m}$  or larger. Fitzsimmons *et al.* (1996) further indicate that  $1$ – $100 \mu\text{m}$  silicate grains will form during the early stages of plume development, while larger grains,  $>500 \mu\text{m}$ , will condense within the cooling fireball. These large particles, however, radiate approximately as blackbodies. The  $10 \mu\text{m}$  emission feature disappears, since variations in  $k$  no longer alter the particle albedo—the particles are already optically thick to radiation. The thermal flux from  $\sim 10 \mu\text{m}$  silicate particles is also shown in Fig. 2.

At  $600$  K (see Fig. 2), aerosols contribute very little radiation in the near infrared, and this drops quickly with decreasing temperatures. Gas emission must be the primary source of the radiation. The  $2.3$  and  $3.3 \mu\text{m}$  methane emission bands ought to be of comparable strength (Strong *et al.* 1993). This is not consistent with the low  $2.3 \mu\text{m}$  fluxes measured by Graham *et al.* and McGregor *et al.*, but is consistent with the Meadows *et al.* measurement.

None of the materials adequately match all of the Sprague *et al.* data, but most of the disagreement is due to gas emission at  $6$ – $8.5 \mu\text{m}$  as stated earlier. The  $4.8$ – $6 \mu\text{m}$  data appear to be continuum emission and would be well matched by a material with constant emissivity and at  $700$ – $800$  K, but aerosols at such temperatures will be far too bright at  $0.9 \mu\text{m}$ . Murchison comes close to the right slope at  $600$  K, but it contributes too much radiation beyond  $11 \mu\text{m}$ . Astronomical silicate is also very neutral and featureless at these wavelengths. Large-grain silicates in sufficient quantity,  $\sim 10^{12}$   $\text{cm}^3$ , come very close to the data as can be seen in Fig. 3 which plots a model containing both small and large silicate aerosols. The inclusion of large-grain silicates degrades the fit to the  $10\text{-}\mu\text{m}$  feature at long wavelengths and does not quite reach the  $4.8$ – $6 \mu\text{m}$  continuum level, but it comes very close, especially considering the large discrepancies seen between data sets. The temperature of this model is very tightly constrained. At temperatures above  $580$  K, the  $0.9 \mu\text{m}$  flux limit is exceeded and below  $580$  K the fit quickly degrades both shortward of  $6 \mu\text{m}$  and longward of  $11 \mu\text{m}$ . Alternatively, there exists a factor of  $\sim 3$  uncertainty in the emissivity of astronomical silicate at  $1$ – $5 \mu\text{m}$  (Draine and Lee 1985), so it also may be possible that small-grain silicates can explain the continuum emission by themselves.

The silicate mass for  $T_a = 350$ – $600$  K is  $\sim 1$ – $5 \times 10^{12}$  g with the higher masses corresponding to lower temperatures. A similar mass of large silicate grains,  $r > 10 \mu\text{m}$ , could be present without being detected. If organic matter is present, it has  $\leq 10\%$  the silicate abundance.

Hammel *et al.* (1995) reported a reflectance of  $I/F = 0.038$  for the E-impact plume. Whereas HST is seeing all the aerosol particles present in the plume, the thermal

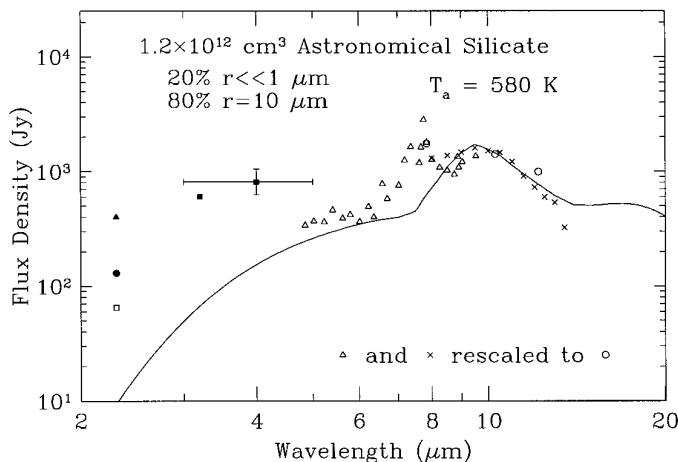


FIG. 3. Thermal emission spectrum of a cloud containing both small and large silicate grains at 580 K. The fit to the 10- $\mu\text{m}$  feature is degraded by the inclusion of the large grains, but now the 4.8–6  $\mu\text{m}$  data are reasonably matched (cf. Fig. 2). Temperatures above 580 K would improve the model but then the flux at 0.9  $\mu\text{m}$  would exceed that measured by Hammel *et al.* (1995). The fit quality quickly worsens at lower temperatures.

infrared observations are primarily sensing those particles taking part in the splash-back at a given time. However, the HST observation was taken several minutes prior to the splash-back phase, so condensation of aerosols was likely still occurring. It is thus difficult to say how the aerosol volume and composition in the plume compare to those in the splash-back phase or later in the blemishes.

An optically thin cloud of aerosols has a reflectance  $I/F = \tau_g Q_s P(\alpha)/4$ , where  $\tau_g$  is the mean geometric optical depth,  $Q_s$  is the particle scattering efficiency, and  $P(\alpha)$  is the particle phase function which for Rayleigh scattering at  $\alpha \approx 0$  has the value 1.5. Assuming a silicate aerosol volume of  $3 \times 10^{11} \text{ cm}^3$  in a  $2 \times 10^6 \text{ km}^2$  plume, aerosols with  $r \approx 0.1 \mu\text{m}$  reproduce the HST reflectance with a scattering optical depth  $\tau_g Q_s = 0.1$ . A comparable volume of large silicate grains would not contribute significantly to the plume's reflectance. Alternatively, if we use the aerosol volume seen in the blemishes ( $4 \times 10^{13} \text{ cm}^3$ ), but scaled down by a factor of 4 to crudely account for the area of the plume still in shadow and material not carried up in the fireball, with  $0.25 \mu\text{m}$  aerosols the plume should be optically thick and extremely reflective. To hide this much material and still be consistent with the infrared observations, the aerosols need radii  $\geq 200 \mu\text{m}$ . It seems more likely that the organic matter simply had not formed yet.

### 3- $\mu\text{m}$ -RING AEROSOL COMPOSITION

McGregor *et al.* (1996) observed the G- and K-impact sites in the near infrared for several hours after the impacts

and in both cases they detected a bright ring expanding beyond the range of the dark blemishes seen in the visible. By the end of Jupiter's first half-rotation the rings faded from view and had radii  $\geq 15,000 \text{ km}$ . The rings were detected in several filters between 3 and 4  $\mu\text{m}$  but not at 2.3  $\mu\text{m}$ . Figure 4 plots the flux spectra of these rings. Because the fluxes decrease with time, measured fluxes for each impact have been interpolated to the time of the first observation in the 3.99  $\mu\text{m}$  filter: 50 min post-impact for G and 35 min for K. These observations encompass the strong 3.3  $\mu\text{m}$  methane absorption band, but the data are not consistent with methane emission. The observed emission peak is at 3.08  $\mu\text{m}$  and no emission was seen at 2.3  $\mu\text{m}$  which is also a strong methane band. The rapid drop in flux away from the maximum at 3.08  $\mu\text{m}$  requires the presence of a material with a very steep change in refractive index in this region.

Many organic solids have an absorption band of varying

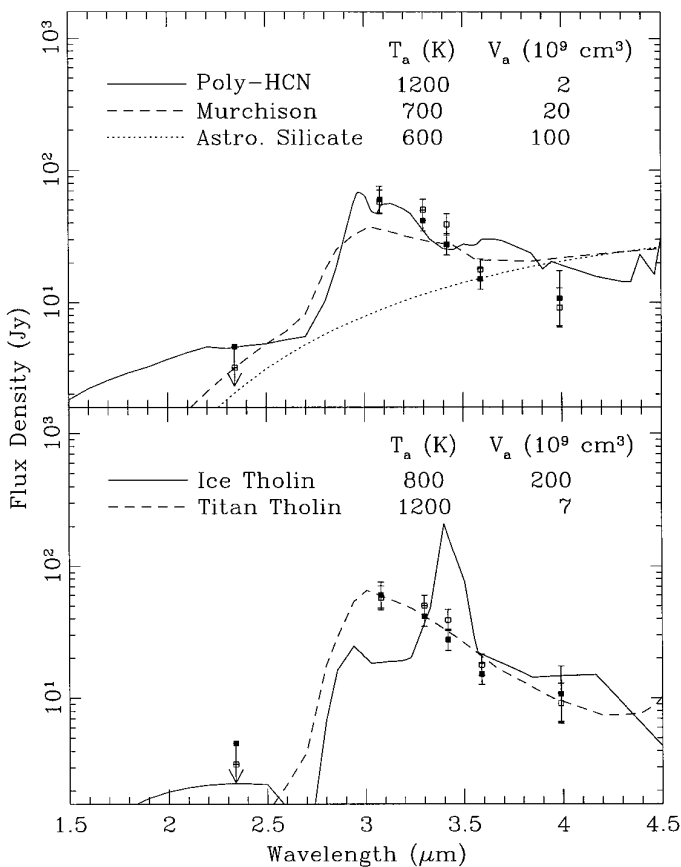


FIG. 4. Comparison of thermal emission from aerosols of five materials with the flux spectrum of the expanding ring seen following the G and K impacts. Primarily because of its large jump in emission efficiency at 3  $\mu\text{m}$ , Titan tholin does the best of all the models. Poly-HCN also does a fair job. [All data from McGregor *et al.* (1996). Solid squares, G impact; open squares, K impact.]

strength at 3  $\mu\text{m}$ . If the radiation from the ring is due to thermal emission instead of reflected sunlight, organic materials can explain this feature. Model flux spectra for the listed temperatures and aerosol volumes of the 5 primary materials from Fig. 1 are plotted in Fig. 4. Titan tholin is by far the best match. Poly-HCN does a fair job but does not have a steep enough dropoff in flux away from 3  $\mu\text{m}$ .

Given the high temperature and low optical depth required to explain the ring, the aerosols should radiatively cool to ambient temperature almost instantly; yet these spectra were obtained 15–30 min after the strong shock-heating of the atmosphere due to the re-entry of ejecta. To have an optically thin cloud retain a temperature of  $\sim 1200$  K for  $>15$  min after the last large thermal event, the aerosols need to be thermally coupled to the surrounding gas which has many orders of magnitude more heat capacity.

At the given temperature and aerosol abundance for the Titan tholin model distributed in a ring  $\sim 10,000$ – $15,000$  km in radius, the ring will be radiating at  $\sim 550$   $\text{erg cm}^{-2} \text{sec}^{-1}$ . An ideal  $\text{H}_2$  atmosphere has a heat capacity of  $6 \times 10^4 (P/1 \mu\text{bar}) \text{erg K}^{-1} \text{cm}^{-2}$ , where  $P$  is the atmospheric pressure at which the aerosols are located, so the gas will be cooled at a rate  $33(1 \mu\text{bar}/P) \text{K hr}^{-1}$ . Therefore, the aerosols must be located at  $P \geq 0.1 \mu\text{bar}$ .

Furthermore, the gas must be able to conduct heat to the aerosols as fast as the aerosols radiate it, which requires a higher gas temperature,  $T_g$ . This heat conduction is given by

$$E = nv\tau_g\Delta u, \quad (2)$$

where  $n$  is the number density of the atmosphere,  $v$  is the mean velocity of particles,  $\tau_g$  is the geometric optical depth (i.e., areal filling factor), and  $\Delta u$  is the energy transferred to an aerosol during each impact which should be at most the difference in a molecule's thermal energy at the two temperatures. Inserting the various thermodynamic quantities and dependency of  $\tau_g$  on aerosol volume and size,  $r$ , gives

$$E = 0.35 \text{ erg cm}^{-2} \text{ sec}^{-1} \left( \frac{P}{1 \mu\text{bar}} \right) \left( \frac{1 \mu\text{m}}{r} \right) \times \left( \frac{1 \text{ K}}{T_g} \right)^{1/2} \left( \frac{T_g - 1200 \text{ K}}{1 \text{ K}} \right). \quad (3)$$

This needs to be greater than  $550 \text{ erg cm}^{-2} \text{ sec}^{-1}$  to balance the outgoing radiation. Solving for  $P$  gives

$$P > 1600 \mu\text{bar} \left( \frac{r}{1 \mu\text{m}} \right) \left( \frac{T_g}{1 \text{ K}} \right)^{1/2} \left( \frac{1 \text{ K}}{T_g - 1200 \text{ K}} \right). \quad (4)$$

An upper limit can also be placed on  $P$  by the need to heat a large amount of atmosphere to a very high temperature. Assuming the entire kinetic energy of a  $10^{14}$ -g impactor were available to heat a 15,000-km radius cylinder of gas down to a pressure of  $P$ ,

$$P < 7000 \mu\text{bar} \left( \frac{1 \text{ K}}{T_g} \right). \quad (5)$$

These two inequalities do not overlap for  $r > 0.05 \mu\text{m}$ . For  $T_g = 1300$ – $2000$  K, the aerosols must have  $r < 0.01$ – $0.04 \mu\text{m}$  and be located at a few microbar. There is contradictory evidence for the size of the Titan tholin aerosols on Titan with radii ranging from 0.03 to  $0.5 \mu\text{m}$  suggested (cf. Toon *et al.* 1992), although  $r$  must certainly be a function of altitude. Under the extremely low pressures at the jovian impact sites, aerosols smaller than  $0.03 \mu\text{m}$  may condense out.

This calculation is the best-case scenario: the entire impactor's energy goes into heating the atmosphere and the excess thermal energy of gas molecules gets transferred with perfect efficiency to the aerosols. Less efficient processes make both inequalities become more restrictive. To maintain overlap, the aerosols need to be even smaller, approximately by the product of the two (in)efficiencies. Very modest inefficiencies drive the aerosol radii below the size of individual molecules ( $\sim \text{nm}$ ). Use of poly-HCN instead of Titan tholin, because of the lower aerosol volume (and optical depth) required, fares even worse in this calculation.

The primary cause of this difficulty is the high temperature required of the aerosols which is determined by fitting the thermal emission of Titan tholin to the 3–4  $\mu\text{m}$  observations of the ring. Titan tholin itself is highly unlikely to be the actual organic produced on Jupiter, since Titan tholin is produced in a 9:1  $\text{N}_2$ : $\text{CH}_4$  atmosphere. This is far removed from the jovian environment. The true jovian tholin will still need to have a well-defined 3- $\mu\text{m}$  feature, but its exact values will differ. If its emissivity drops at longer wavelengths faster than Titan tholin, a lower temperature will be possible. In addition to not needing as hot an atmosphere, the aerosol optical depth will significantly increase, improving heat conduction.

#### COMETARY DELIVERY OR *IN SITU* SYNTHESIS?

The silicates observed in the blemishes must come from the impact fragments. The organic matter, however, could be either (1) deposited by the impacting object, (2) quench-synthesized from cometary dissociation products, or (3) shock-synthesized from the jovian atmosphere. To determine the feasibility of these three models we estimate the quantity of organics available from these sources and

compare it to the masses calculated in the previous sections.

Although there remains significant uncertainty in impactor sizes, models are converging on  $\sim 500$ -m-diameter fragments with the larger fragments having masses of  $\sim 10^{14}$  g (Asphaug and Benz 1996). Assuming a cometary composition of 20–25% organic matter (Chyba *et al.* 1990, Greenberg and Hage 1990), up to  $\sim 2 \times 10^{13}$  g of organic matter will be delivered by an impactor. This is within the range needed to produce the blemishes if the aerosols have porosities  $\geq 80\%$ . However, the organic matter must survive the airburst and the high temperatures of the rising plume. The hardest organic materials are unable to survive temperatures above 2000 K for more than 1 sec (Chyba *et al.* 1990). The temperature of the fireball was initially  $T \geq 10^4$  K (Martin *et al.* 1995) and remained above 2000 K for  $\geq 15$  sec (Carlson *et al.* 1995), so only a small fraction of material (perhaps that ablated off the fragments well before the actual airburst) would be expected to avoid destruction. To survive the fireball and be seen, the object would need to fragment into pieces small enough to be carried upward by the hot rising gases, but large enough to survive evaporation until the temperature drops significantly below 2000 K, thereby protecting the inner material. Although observations of the plume and splash-back are consistent with  $\sim 4 \times 10^{13}$  cm<sup>3</sup> of matter in the form of  $>200$ - $\mu$ m particles, it seems highly improbable that so much of the impactor could escape vaporization and that each grain would then on re-entry shatter into  $\sim 10^9$  0.25- $\mu$ m aerosol particles.

Cometary material that is vaporized and dissociated in the fireball will recombine into new products as the rising plume cools. Laser-pulse heating of meteorites suggests that most of the impactor's carbon will be converted to CO and CO<sub>2</sub>, regardless of the surrounding atmosphere (Mukhin *et al.* 1989). About 20% of the carbon will end up in hydrocarbons, of which  $\sim 5\%$  will contain 3 or more carbon atoms (Mukhin *et al.* 1989). A vaporized  $10^{14}$ -g comet can thus produce  $\sim 10^{12}$  g of heavy hydrocarbons and organics. This is less than the  $\geq 10^{13}$  g needed for the blemishes, but there are large uncertainties in extrapolating the experimental data to the SL-9 impacts. Laboratory experiments can produce only very-short-duration and low-mass-vapor events. Mukhin *et al.* used laser pulses of  $\sim 10^{-3}$  sec duration which vaporized  $\sim 10$  mg of meteoritic material. The chemistry within the vapor plume of a  $10^{14}$ -g comet cooling over a period of minutes is likely to differ in both species production and conversion efficiency. Unlike the preceding case of organics surviving the airburst and fireball, the quench-synthesis mechanism is certain to contribute some organics.

When the impactor airbursts, its kinetic energy goes into a shock wave that heats the surrounding atmosphere and converts some of the methane and ammonia into complex

organic matter. Shock synthesis of organic matter in a reducing atmosphere is a highly efficient process (Bar-Nun *et al.* 1970). The relevant laboratory experiments simulating shock synthesis of organic solids in a jovian atmosphere, though, have not been performed. The most analogous experiment that *has* been performed is the charged-particle irradiation of a near-jovian atmosphere composed of 85% H<sub>2</sub>, 13% He, 1% CH<sub>4</sub>, and 1% NH<sub>3</sub> which gives a tholin production efficiency of  $\eta = 10^{-15}$  g erg<sup>-1</sup> (McDonald *et al.* 1992). Laser-induced plasmas, which create conditions similar to those of shock waves, are several times more efficient than charged-particle irradiation at producing gaseous organic molecules (Scattergood *et al.* 1989). Assuming this also applies to production of the organic solid, the shock-synthesis value of  $\eta$  could be  $\sim 3$  times larger. Further, because the methane and ammonia in the McDonald *et al.* (1992) experiment are overabundant by factors of  $\sim 10$ , the true jovian  $\eta$  will be lower than that measured. The production of complex organic matter scales with methane abundance as  $\sim X_{\text{CH}_4}^{0.5}$  (Thompson *et al.* 1987, 1994, Khare *et al.* 1987), so the final production efficiency is estimated as  $\eta \approx 10^{-15}$  g erg<sup>-1</sup>. There remains considerable uncertainty in this estimate, though. Given the much higher energy and longer cooling time scale in the jovian shock wave than those simulated in the lab,  $\eta$  could easily be off by a factor  $>10$ . The introduction of other species, perhaps acting as catalysts for certain reactions, from the impactors further complicates the issue.

The energy of a  $10^{14}$ -g impactor striking Jupiter at 60 km sec<sup>-1</sup> is  $2 \times 10^{27}$  erg. The mass of tholin possibly produced is, therefore,  $\sim 2 \times 10^{12}$  g. This is insufficient mass to produce the blemishes. Furthermore, in an atmosphere highly diluted with H<sub>2</sub> and He, organic solids are not the most abundant product of shock synthesis. In fact, almost 1000 times more gaseous organic molecules should be produced than solids (McDonald *et al.* 1992), a large fraction of which is likely to be in the form of HCN gas (Scattergood *et al.* 1989). Theoretical models of shock synthesis place a strong upper limit of  $4 \times 10^{-16}$  g erg<sup>-1</sup> for the production efficiency of HCN in a jovian atmosphere (Lewis 1980). This is consistent with the  $\leq 10^{12}$  g of HCN observed in individual impacts (Marten *et al.* 1995, Bezar *et al.* 1997). If there is no very efficient conversion of HCN to organic solids (e.g., poly-HCN), only  $\sim 10^9$  g of organic solids may be produced. Although this is vastly insufficient to produce the dark blemishes, it is very close to the mass of either poly-HCN or tholin required to explain the bright expanding ring.

## DISCUSSION

In this study we have used observations of the plume, the thermal pulse during ejecta re-entry, the post-impact blemishes, and the large expanding ring seen only in the

infrared to search for clues about the composition of the aerosols seen at each phase. Small silicate grains are adequate to explain the solar reflectance of the initial plumes and the 10  $\mu\text{m}$  feature seen at peak brightness. The aerosol size required to explain both observations, given a total volume  $3 \times 10^{11} \text{ cm}^3$ , is  $r = 0.1 \mu\text{m}$ . At temperatures consistent with the low flux of the E plume at 0.9  $\mu\text{m}$ , these aerosols cannot reproduce the fluxes measured below 8  $\mu\text{m}$ . Most of these observations, however, coincide with methane and water vapor emission bands. Adding  $\sim 10^{12} \text{ cm}^3$  of large-grain ( $>10 \mu\text{m}$ ) silicates, or adopting an emissivity for the small-grain silicates  $\sim 3$  times greater than used here, produces a fair match to the continuum emission seen at 5–6  $\mu\text{m}$ .

Murchison organic residue is an excellent match to the well-sampled imaginary refractive index data of the blemish aerosols from 0.3 to 1.0  $\mu\text{m}$ . Poly-HCN may likewise work but the aerosols need to be highly porous, perhaps due to coagulation of the initial condensation nuclei. Poly-HCN may be expected as a product from the shocked jovian atmosphere, but probably not in sufficient quantities. Alternatively, Fischer–Tropsch-type reactions within the cooling fireball may be a source of organics (G. Field, personal communication, 1995). Although it has been hypothesized that Murchison organics were produced by Fischer–Tropsch reactions in the solar nebula (Hayatsu and Anders 1981) and therefore may be a good analogue for the organics produced in the plume, isotopic and molecular discrepancies have brought this proposed origin for meteoritic organics (Cronin and Chang 1993) into serious question. Thus we cannot test this hypothesis using spectrophotometry of the blemishes.

For an impactor mass of  $10^{14} \text{ g}$ , none of the three methods seems quite capable of producing the blemishes. Although cometary fragments contain enough organic matter and will deliver into Jupiter's atmosphere at least an order of magnitude more organic material than can be shock-synthesized from the atmosphere or quench-synthesized from the cooling fireball, the intense heat of the fireball seems likely to destroy most of the indigenous organics. Given the extraordinary match between Murchison organic residue and the aerosol optical constants, it is tempting to believe that somehow indigenous cometary organics survived the fireball, but the contortions required are too great. The failure of atmospheric tholins to model the aerosols and the extremely low HCN abundance seen at the impact sites also serve as significant obstacles to a shock-synthesized origin. Quench synthesis falls an order of magnitude short of the blemish masses, but given the extrapolation of laboratory data over 16 orders of magnitude in mass and 5 orders of magnitude in time, an uncertainty of one order of magnitude seems quite modest.

## ACKNOWLEDGMENTS

This research was supported by NASA Grants NAGW 1870 and NAGW 1896. P.W. was supported by the NASA Graduate Student Researchers Program. We thank Peter McGregor, Philip Nicholson, and Ann Sprague for access to their data and J. L. Ortiz and A. Bar-Nun for helpful reviews.

## REFERENCES

- Asphaug, E., and W. Benz 1996. Size, density, and structure of Comet Shoemaker–Levy 9 inferred from the physics of tidal breakup. *Icarus* **121**, 225–248.
- Banfield, D., P. J. Gierasch, S. W. Squyres, and P. D. Nicholson 1996. 2  $\mu\text{m}$  spectrophotometry of jovian stratospheric aerosols—scattering opacities, vertical distributions, and wind speeds. *Icarus* **121**, 389–410.
- Bar-Nun, A., N. Bar-Nun, S. H. Bauer, and C. Sagan 1970. Shock synthesis of amino acids in simulated primitive environments. *Science* **168**, 470–473.
- Bézar, B., C. A. Griffith, D. M. Kelly, J. H. Lacy, T. Greathouse, and G. Orton 1997. Thermal infrared imaging spectroscopy of Shoemaker–Levy 9 impact sites: Temperature and HCN retrievals. *Icarus* **125**, 94–120.
- Carlson, R. W., P. R. Weissman, M. Segura, J. Hui, W. D. Smythe, T. V. Johnson, K. H. Baines, P. Drossart, Th. Encrenaz, and F. E. Leader 1995. Galileo infrared observations of the Shoemaker–Levy 9 G impact fireball: A preliminary report. *Geophys. Res. Lett.* **22**, 1557–1560.
- Chyba, C. F., P. J. Thomas, L. Brookshaw, and C. Sagan 1990. Cometary delivery of organic molecules to the early Earth. *Science* **249**, 366–373.
- Cronin, J. R., and S. Chang 1993. Organic matter in meteorites: Molecular and isotopic analyses of the Murchison meteorite. In *The Chemistry of Life's Origins* (J. M. Greenberg, C. X. Mendoza-Gomez, and V. Pirronello, Eds.), pp. 209–258. Kluwer Academic, Netherlands.
- Draine, B. T. 1985. Tabulated optical properties of graphite and silicate grains. *Astrophys. J. Suppl.* **57**, 587–594.
- Draine, B. T., and H. M. Lee 1984. Optical properties of interstellar graphite and silicate grains. *Astrophys. J.* **285**, 89–108.
- Fitzsimmons, A., P. J. Andrews, R. Catchpole, J. E. Little, N. Walton, and I. P. Williams 1996. Re-entry and ablation of cometary dust in the impact plumes of Shoemaker–Levy 9. *Nature* **379**, 801–804.
- Friedson, A. J., W. F. Hoffmann, J. D. Goguen, L. K. Deutsch, G. S. Orton, J. L. Hora, A. Dayal, J. N. Spitale, W. K. Wells, and G. G. Fazio 1995. Thermal infrared lightcurves of the impact of Comet Shoemaker–Levy 9 fragment R. *Geophys. Res. Lett.* **22**, 1569–1572.
- Graham, J. R., I. de Pater, J. G. Jernigan, M. C. Liu, and M. E. Brown 1995. The fragment R collision: W. M. Keck telescope observations of SL9. *Science* **267**, 1320–1323.
- Greenberg, J. M., and J. I. Hage 1990. From interstellar dust to comets: A unification of observational constraints. *Astrophys. J.* **361**, 260–274.
- Hammel, H. B., R. F. Beebe, A. P. Ingersoll, G. S. Orton, J. R. Mills, A. A. Simon, P. Chodas, J. T. Clarke, E. De Jong, T. E. Dowling, J. Harrington, L. F. Huber, E. Karkoschka, C. M. Santori, A. Toigo, D. Yeomans, and R. A. West 1995. HST imaging of atmospheric phenomena created by the impact of Comet Shoemaker–Levy 9. *Science* **267**, 1288–1296.
- Hayatsu, R., and E. Anders 1981. Organic compounds in meteorites and their origins. *Top. Curr. Chem.* **99**, 1–37.
- Khare, B. N., C. Sagan, E. T. Arakawa, F. Suits, T. A. Callcott, and M. W. Williams 1984. Optical constants of organic tholins produced in a simulated titanian atmosphere: From soft X-ray to microwave frequencies. *Icarus* **60**, 127–137.

- Khare, B. N., C. Sagan, W. R. Thompson, E. T. Arakawa, and P. Votaw 1987. Solid hydrocarbon aerosols produced in simulated uranian and neptunian stratospheres. *J. Geophys. Res.* **92**, 15067–15082.
- Khare, B. N., W. R. Thompson, L. Cheng, C. F. Chyba, C. Sagan, E. T. Arakawa, C. Meisse, and P. S. Tuminello 1993. Production and optical constants of ice tholin from charged particle irradiation of (1:6) C<sub>2</sub>H<sub>6</sub>/H<sub>2</sub>O at 77 K. *Icarus* **103**, 290–300.
- Khare, B. N., W. R. Thompson, C. Sagan, E. T. Arakawa, C. Meisse, and I. Gilmour 1990. Optical constants of kerogen from 0.15 to 40 μm: Comparison with meteoritic organics. In *First International Conference on Laboratory Research for Planetary Atmospheres* (K. Fox, J. E. Allen, Jr., L. J. Stief, and D. T. Quillen, Eds.), NASA Conference Publication 3077, pp. 340–356. NASA, Washington, DC.
- Lewis, J. S. 1980. Lightning synthesis of organic compounds on Jupiter. *Icarus* **43**, 85–95.
- Marten, A., D. Gautier, M. J. Griffin, H. E. Matthews, D. A. Naylor, G. R. Davis, T. Owen, G. Orton, D. Bockelée-Morvan, P. Colom, J. Crovisier, E. Lellouch, I. de Pater, S. Atreya, D. Strobel, B. Han, and D. B. Sanders 1995. The collision of Comet Shoemaker–Levy 9 with Jupiter: Detection and evolution of HCN in the stratosphere of the planet. *Geophys. Res. Lett.* **22**, 1589–1592.
- Martin, T. Z., G. S. Orton, L. Travis, L. Tamppari, and I. Claypool 1995. Observation of Shoemaker–Levy impacts by the Galileo photopolarimeter radiometer. *Science* **268**, 1875–1879.
- Matthews, C. N. 1992. Dark matter in the Solar System: Hydrogen cyanide polymers. *Origins Life* **21**, 421–434.
- Matthews, C. N. 1994. Hydrogen cyanide polymers from the impact of Comet Shoemaker–Levy 9 on Jupiter. *Bull. Am. Astron. Soc.* **26**, 1587.
- McDonald, G. D., W. R. Thompson, and C. Sagan 1992. Radiation chemistry in the jovian stratosphere: Laboratory simulations. *Icarus* **99**, 131–142.
- McGregor, P. J., P. D. Nicholson, and M. G. Allen 1996. CASPIR observations of the collision of Comet Shoemaker–Levy 9 with Jupiter. *Icarus* **121**, 361–388.
- Meadows, V., D. Crisp, G. Orton, T. Brooke, and J. Spencer 1995. AAT IRIS observations of the SL-9 impacts and initial fireball evolution. In *Proceedings of the European SL-9/Jupiter Workshop* (R. West and H. Bohnhardt, Eds.), pp. 129–134. ESO, Garching.
- Moreno, F., O. Muñoz, A. Molina, J. J. López-Moreno, J. L. Ortiz, J. Rodríguez, A. López-Jiménez, F. Girela, S. M. Larson, and H. Campins 1995. Physical properties of the aerosol debris generated by the impact of fragment H of Comet P/Shoemaker–Levy 9 on Jupiter. *Geophys. Res. Lett.* **22**, 1609–1612.
- Mukhin, L. M., M. V. Gerasimov, and E. N. Safonova 1989. Origin of precursors of organic molecules during evaporation of meteorites and mafic terrestrial rocks. *Nature* **340**, 46–48.
- Muñoz, O., F. Moreno, and A. Molina 1996. Aerosol properties of debris from fragments E/F of Comet Shoemaker–Levy 9. *Icarus* **121**, 305–310.
- Nicholson, P. D., P. J. Gierasch, T. L. Hayward, C. A. McGhee, J. E. Moersch, S. W. Squyres, J. Van Cleve, K. Matthews, G. Neugebauer, D. Shupe, A. Weinberger, J. W. Miles, and B. J. Conrath 1995a. Palomar observations of the R impact of Comet Shoemaker–Levy 9: I. Light curves. *Geophys. Res. Lett.* **22**, 1613–1616.
- Nicholson, P. D., P. J. Gierasch, T. L. Hayward, C. A. McGhee, J. E. Moersch, S. W. Squyres, J. Van Cleve, K. Matthews, G. Neugebauer, D. Shupe, A. Weinberger, J. W. Miles, and B. J. Conrath 1995b. Palomar observations of the R impact of Comet Shoemaker–Levy 9: II. Spectra. *Geophys. Res. Lett.* **22**, 1617–1620.
- Ortiz, J. L., O. Muñoz, F. Moreno, A. Molina, T. M. Herbst, K. Birkle, H. Böhnhardt, and D. P. Hamilton 1995. Models of the SL-9 collision-generated hazes. *Geophys. Res. Lett.* **22**, 1605–1608.
- Rosenqvist, J., Y. G. Biraud, M. Cuisenier, A. Marten, T. Hidayat, G. Chountonov, D. Moreau, C. Muller, I. Maslov, M. Ackerman, Y. Ballega, and O. Korablev 1995. Four micron infrared observations of the Comet Shoemaker–Levy 9 collision with Jupiter at the Zelenchuk Observatory: Spectral evidence for a stratospheric haze and determination of its physical properties. *Geophys. Res. Lett.* **22**, 1585–1588.
- Roush, T., J. Pollack, and J. Orenberg 1991. Derivation of midinfrared (5–25 μm) optical constants of some silicates and palagonite. *Icarus* **94**, 191–208.
- Sagan, C., W. R. Thompson, and B. N. Khare 1992. Titan: A laboratory for prebiological organic chemistry. *Accs. Chem. Res.* **25**, 286–292.
- Scattergood, T. W., C. P. McKay, W. J. Borucki, L. P. Giver, and H. Van Ghysseghem 1989. Production of organic compounds in plasmas: A comparison among electric sparks, laser-induced plasmas, and UV light. *Icarus* **81**, 413–428.
- Sprague, A. L., G. L. Bjoraker, D. M. Hunten, F. C. Witteborn, R. W. H. Kozlowski, and D. H. Wooden 1996. Water brought into Jupiter's atmosphere by fragments R and W of Comet SL-9. *Icarus* **121**, 30–37.
- Strong, K., F. W. Taylor, S. B. Calcutt, J. J. Remedios, and J. Ballard 1993. Spectral parameters of self- and hydrogen-broadened methane from 2000 to 9500 cm<sup>-1</sup> for remote sounding of the atmosphere of Jupiter. *J. Quant. Spectros. Rad. Transfer* **50**, 363–429.
- Thompson, W. R., T. Henry, B. N. Khare, L. Flynn, J. Schwartz, and C. Sagan 1987. Light hydrocarbons from plasma discharge in H<sub>2</sub>–He–CH<sub>4</sub>: First results and uranian auroral chemistry. *J. Geophys. Res.* **92**, 15,083–15,092.
- Thompson, W. R., G. D. McDonald, and C. Sagan 1994. The Titan haze revisited: Magnetospheric energy sources and quantitative tholin yields. *Icarus* **112**, 376–381.
- Toon, O. B., C. P. McKay, C. A. Griffith, and R. P. Turco 1992. A physical model of Titan's aerosols. *Icarus* **95**, 24–53.
- West, R. A., E. Karkoschka, A. J. Friedson, M. Seymour, K. H. Baines, and H. B. Hammel 1995. Impact debris particles in Jupiter's stratosphere. *Science* **267**, 1296–1301.
- Wilson, P. D., and C. Sagan 1995. Spectrophotometry and organic matter on Iapetus. 1. Composition models. *J. Geophys. Res.-Planets* **100**, 7531–7537.
- Wilson, P. D., C. Sagan, and W. R. Thompson 1994. The organic surface of 5145 Pholus: Constraints set by scattering theory. *Icarus* **107**, 288–303.
- Yelle, R. V., and M. A. McGrath 1996. Ultraviolet spectroscopy of the SL9 impact sites. *Icarus* **119**, 90–111.